2016

A dual deformation mechanism of grain boundary at different stress stages

Liang Zhang
University of Wollongong, lz592@uowmail.edu.au

Cheng Lu
University of Wollongong, chenglu@uow.edu.au

Jie Zhang
University of Wollongong, jz248@uowmail.edu.au

A Kiet Tieu
University of Wollongong, ktieu@uow.edu.au

Publication Details

Zhang, L., Lu, C., Zhang, J. & Tieu, K. (2016). A dual deformation mechanism of grain boundary at different stress stages. Materials Letters, 167 278-283.

A dual deformation mechanism of grain boundary at different stress stages

Abstract
Molecular dynamics (MD) simulation with embedded-atom method (EAM) potential was carried out to study the structure and shear response of an asymmetric tilt grain boundary in copper bicrystal. A non-planar structure with dissociated intrinsic stacking faults was observed in the grain boundary. Simulation results show that this type of structure can significantly increase the ductility of the simulation sample under shear deformation. A dual deformation mechanism of the grain boundary was observed; the grain boundary can be a source of dislocation emission and migrate itself at different stress stages. The result of this study can provide further information to understand the grain boundary mediated plasticity in nanocrystalline materials.

Disciplines
Engineering | Science and Technology Studies

Publication Details
Zhang, L., Lu, C., Zhang, J. & Tieu, K. (2016). A dual deformation mechanism of grain boundary at different stress stages. Materials Letters, 167 278-283.

A dual deformation mechanism of grain boundary at different stress stages

Liang Zhang, Cheng Lu*, Jie Zhang, Kiet Tieu

School of Mechanical, Materials and Mechatronic Engineering, University of Wollongong, Wollongong, NSW 2522, Australia.

*Corresponding author. Tel.:+6144214639; fax:+61242213101;

E-mail: chenglu@uow.edu.au (C. Lu)

Abstract: Molecular dynamics (MD) simulation with embedded-atom method (EAM) potential was carried out to study the structure and shear response of an asymmetric tilt grain boundary in copper bicrystal. A non-planar structure with dissociated intrinsic stacking faults was observed in the grain boundary. Simulation results show that this type of structure can significantly increase the ductility of the simulation sample under shear deformation. A dual deformation mechanism of the grain boundary was observed; the grain boundary can be a source of dislocation emission and migrate itself at different stress stages. The result of this study can provide further information to understand the grain boundary mediated plasticity in nanocrystalline materials.

Keywords: Grain boundary; Dislocation; Shear deformation; Plasticity

1. Introduction

Compared with conventional coarse-grained materials, nanocrystalline materials show a lot of advanced performances[1, 2], which stimulated widespread interest in the mechanical properties and novel deformation mechanisms of nano-sized materials. The deformation mechanisms of metals with the average grain size in the nanometer range are studied extensively in the past two decades[3, 4]. Grain boundary (GB) has been confirmed to play an important role in the mechanical behavior of nanocrystalline metals by both experimental observations and atomistic simulations. The identified deformation mechanisms in nanocrystalline metals include GB sliding[5, 6], grain rotation[7-9], GB migration[10-13], dislocation sink in or nucleate from GBs[14-16].

Most of the previous work show that single deformation mechanism can be activated for a certain GB. For example, by using molecular dynamics (MD) simulation, Qi and Krajewski[6] showed that GB sliding is the primary deformation mechanism in bicrystal Al under a shear force. Cahn et al.[9] found that all of the <0 0 1> symmetric tilt GBs in Cu can migrate coupled to a shear deformation. Zhang et al.[16] observed that dislocation nucleation dominant the mechanism of a deformed Cu with <1 1 0> symmetric tilt GBs under tension. By using the quasi-continuum method, Sansoz and Molinari[17] correlated individual failure mechanisms to certain GBs. In tension, failure of the GBs occurred via partial dislocation nucleation and GB cleavage. In shear, they reported three different failure modes depending on the boundary structures: GB sliding by atomic shuffling, nucleation of partial dislocations from GB, and GB migration. To the best of the author's knowledge, a dual deformation mechanism of the same GB has

rarely reported previously. Also, the computer modeling of GBs has been mostly focused on symmetrical GBs, which possess mirror symmetry of crystallographic planes. In contrast, very few atomistic simulations have been conducted on the asymmetric GBs. In this study, we reported a Σ11 asymmetric GB with a non-planar structure that can play a role as dislocation source and migrate itself at different stress stages under shear deformation.

2. Methodology

Molecular dynamics simulation was carried out to study Σ11(2 2 5)/(4 4 1) Φ=54.74° asymmetric tilt GB in Cu bicrystal. The simulation was carried out using the parallel molecular dynamics code LAMMPS[18] with the embedded-atom method (EAM) potential for Cu developed by Mishin et al.[19]. A bicrystal model was created by constructing two separate crystal lattices with different crystallographic orientation and joining them together along the Y axis (see Fig.1). A periodic boundary condition was applied in the X and Z directions while a non-periodic boundary condition was applied in the Y direction. The equilibrium structure of the GB was obtained by the energy minimization procedure and the subsequent MD relaxation in the isobaric-isothermal (NPT) ensemble at a pressure of 0 bar and a temperature of 300 K for 20 ps. As shown in the atomic configuration in Fig.1, the equilibrium Σ11(Φ=54.74°) asymmetric GB shows an obvious non-planar structure with an intrinsic stacking fault that dissociated from the boundary plane.

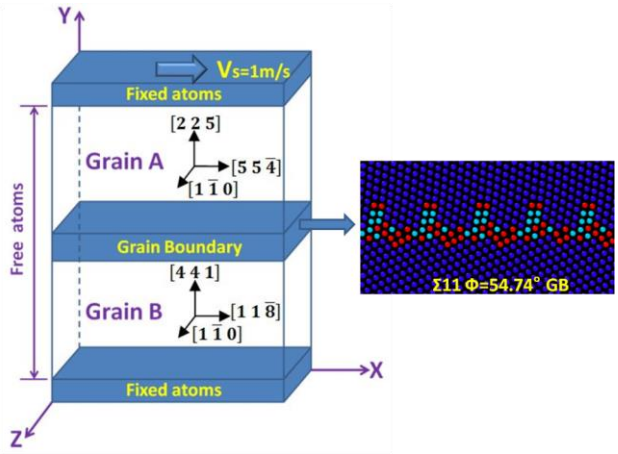

Fig.1 Schematic of the simulation model. A constant shear velocity V_s=1m/s parallel to the boundary plane was applied during the shear deformation. The atomic configuration shows the equilibrium structure of the Σ11(2 2 5)/(4 4 1) (Φ=54.74°) asymmetric GB. The images are viewed along the [1 $\bar{1}$ 0] tilt axis and are colored according to the common neighbor analysis (CNA) parameter. Atoms with perfect fcc structures are colored with blue, the red atoms represent the GB plane and the dislocation core, the light blue atoms represent the stacking fault.

Once the equilibrium state of GB was reached, a shear deformation was applied to bicrystal model. Atoms on the top of grain-A and atoms at the bottom of grain-B were fixed, the thickness of each fixed slab was approximate twice the cutoff radius of atomic interactions[10], while all the other atoms in the model were set free. A constant shear velocity V_s=1m/s (about 4.6×10^7/s shear strain) parallel to the boundary plane was

applied to the fixed area of grain-A in the +X direction. Throughout the MD simulation, the NPT ensemble was adopted and the time increment of simulations was fixed at 1 fs. Stress and temperature calculations were performed on the dynamic atoms between the two fixed slabs. In atomic level, the stress is computed according to the virial theorem by the formula:

$$\sigma_{ij} = \frac{1}{V}\sum_{\alpha=1}^{N}\left(\frac{1}{2}\sum_{\beta=1}^{N} r_{\alpha\beta}^{i} F_{\alpha\beta}^{j} - m^{\alpha}\, v_{i}^{\alpha} v_{j}^{\alpha}\right) \qquad (1)$$

Where *i*, *j* are Cartesian coordinates and α and β are atom index numbers. *m* and *v* denote to the mass and velocity of the atom. $r_{\alpha\beta}$ and $F_{\alpha\beta}$ are respectively the distance and force between two atoms with index α and β. *V* is the volume of the system and with number of total atoms *N*.

Generally, if a dislocation is subjected to stress, it tends to move through the crystal. This motion is the mechanism for plastic flow in a crystalline solid. The tendency of a dislocation to move can be described by Peach-Koehler formula[20], which states that the driving force for dislocation motion can be computed from the following equation:

$$\boldsymbol{F_L} = \left(\boldsymbol{b} \cdot \sigma_{ij}\right) \times \boldsymbol{\xi} \qquad (2)$$

where $\boldsymbol{F_L}$ is the force per unit length of dislocation, this is essentially *F/L* for a straight dislocation where *L* is the length of the dislocation line; $\boldsymbol{b}$ is Burger vector of a given dislocation; σ_{ij} is the stress tensor and $\boldsymbol{\xi}$ is the line vector of the dislocation. For a mixed dislocation (with both screw and edge characteristics) of which the tangent to the dislocation line is neither parallel or perpendicular to the Burgers vector, let $\boldsymbol{b} = (b_x\ b_y\ b_z)$, $\boldsymbol{\xi} = (\xi_x\ \xi_y\ \xi_z)$ and $\boldsymbol{g} = \boldsymbol{b} \cdot \boldsymbol{\sigma_{ij}}$, then:

$$g_x = b_x\sigma_{xx} + b_y\tau_{xy} + b_z\tau_{xz}$$

$$g_y = b_x\tau_{yx} + b_y\sigma_{yy} + b_z\tau_{yz}$$

$$g_z = b_x\tau_{zx} + b_y\tau_{zy} + b_z\sigma_{zz} \qquad (3)$$

and

$$\boldsymbol{F_L} = \boldsymbol{g} \times \boldsymbol{\xi} = \begin{vmatrix} i & j & k \\ g_x & g_y & g_z \\ \xi_x & \xi_y & \xi_z \end{vmatrix} \qquad (4)$$

This general form of the Peach-Koehler equation is used to calculate the magnitudes of the forces on and the forces between dislocations.

3. Result and discussion

The shear stress of the bicrystal model with Σ11(2 2 5)/(4 4 1) GB as a function of shear strain was plotted in Fig.2. The deformation of the bicrystal model occurred in four stages: elastic, plastic, strain-hardening and strain-softening. These stages were divided by the dashed line in Fig.2. The corresponding deformation configurations were presented in Fig.3(a). The *Crystal Analysis Tool*[21, 22] was used to detect dislocations

in this study. The identified dislocations were converted into continuous lines and their Burgers vectors were calculated, as shown in Fig.3(b).

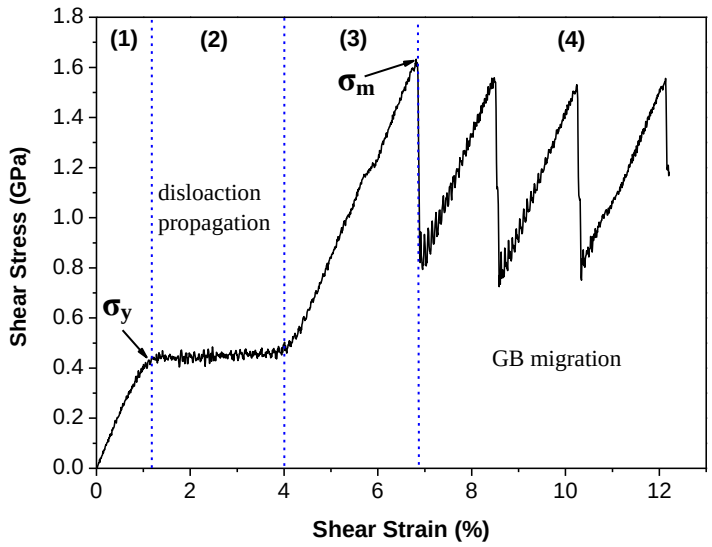

Fig.2 The shear response of Cu bicrystal model with Σ11(2 2 5)/(4 4 1) Φ=54.74° asymmetric tilt GB at 300 K. The four deformation stages are indexed by (1) elastic (2) plastic (3) strain-hardening and (4) strain-softening.

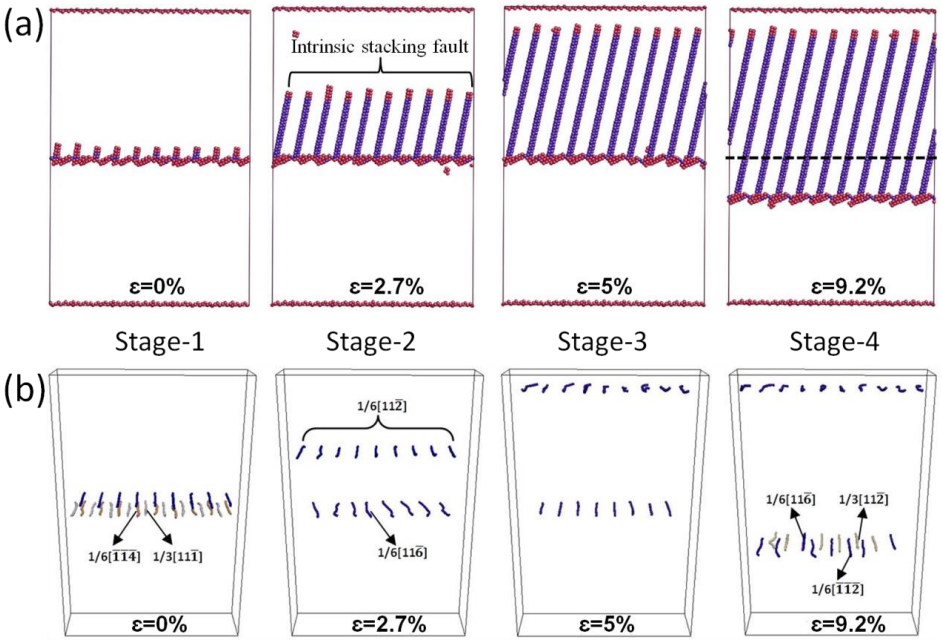

Fig.3 Snapshots of Cu bicrystal model at different deformation stages. (a) shows the results from MD simulation. The atoms with perfect FCC structure are removed to facilitate the view of the GB and dislocation structures. (b) shows the extracted dislocation segment by using the Crystal Analysis Tool.

In the elastic stage, the GB structure kept its initial equilibrium configuration. The simulation results indicate that the equilibrium boundary structure can be regarded as

being composed of an array of GB dislocations with Burgers vector **b**=(1/6)[$\bar{1}\ \bar{1}\ \bar{4}$] and **b**=(1/3)[1 1 $\bar{1}$], along with the dissociated Shockley partial dislocations extended from the boundary plane. With the increasing of shear deformation, the dissociated Shockley partial dislocations began to emit from the GB plane with an extension of the intrinsic stacking fault behind, resulting in the plastic deformation stage (see Fig.3(a) at ε=2.7%). Visual inspection of the simulation results, it can be found that the dissociated Shockley partial dislocations from GB plane are nearly pure edges with the dislocation lines along the Z direction, and therefore, had Burgers vectors with large y-components and small x-components. As a simplification for this case, we consider the simulation as a shear force acting on an array of straight edge dislocations with $\boldsymbol{b} = (0\ 1\ 0)$ and $\boldsymbol{\xi} = (0\ 0\ 1)$, according to Eq.(3),

$$\boldsymbol{g} = b\begin{vmatrix}\sigma_{xx} & \tau_{xy} & \tau_{xz}\\ \tau_{yx} & \sigma_{yy} & \tau_{yz}\\ \tau_{zx} & \tau_{zy} & \sigma_{zz}\end{vmatrix}\begin{vmatrix}0\\1\\0\end{vmatrix} = b|\tau_{xy} \quad \sigma_{yy} \quad \tau_{zy}| \qquad (5)$$

and according to Eq.(4), taking the cross product of $\boldsymbol{g}$ and the line sense $\boldsymbol{\xi}$ we get:

$$\boldsymbol{F_L} = \boldsymbol{g} \times \boldsymbol{\xi} = \begin{vmatrix} i & j & k\\ b\tau_{xy} & b\sigma_{yy} & b\tau_{zy}\\ 0 & 0 & 1\end{vmatrix}$$

$$= b\sigma_{yy}\, i - b\tau_{xy} j = b\sigma_{yy}\, i + b\tau_{yx} j = F_x + F_y \qquad (6)$$

Eq.(6) indicates that only τ_{yx} and σ_{yy} can exert force on these dissociated dislocations and that the force acts normal to the dislocation line along its length. F_x is the climbing force in the +X direction while F_y is the glide force acting in the +Y direction. In general, dislocation climb requires higher thermal activation energy, which is hard to occur at an ambient temperature. Therefore, it is reasonable to observe the dissociated dislocations slip upwards that driven by the applied shear stress (τ_{yx}) in grain-A. Moreover, the interaction of the parallel edge dislocations has been neutralized since both of them have the identical Burgers vector, and the distance between them are equal.

Note that the comparative low yield stress (σ_y=0.42 GPa) was mainly due to the intrinsic GB structure with the embryo dissociated dislocations (see in Fig.1) where only a low-level stress can drive them to emit. Also, it is interesting to see that the stress curve reached a plateau in the plastic stage, indicating that the slipping of dislocations in grain-A played a small role in accommodating the system stress. This was different from the previous finding where the stress curve started to drop once the dislocation became active[10, 16, 17]. As mentioned previously, these partial dislocations were pure edges which have Burgers vectors with large y-components and small x-components. Consequently, the region swept by this array in grain-A had undergone a tilt rotation and suffered a misfit strain. This distortion significantly altered the local stress distributions, causing the stress distribution to become very nonuniform. Once this had occurred, the stress-strain curve in stage-2 bears essentially no physical significance in depicting the stresses within the models. Therefore, the dislocation movement did not reduce the

stress value. Instead, the stress curve plateaued in the plastic stage. To visually display the stress distribution in the bicrystal system, the Von Mises stress of each atom in the simulation system was calculated by using Eq.(7) and the results were shown in Fig.4. Atoms with the stress value less than 1.5 GPa were removed to facilitate the view of stress change within the simulation system.

$$\sigma_{ij} = \sqrt{1/2[(\sigma_{xx} - \sigma_{yy})^2 + (\sigma_{yy} - \sigma_{zz})^2 + (\sigma_{zz} - \sigma_{xx})^2 + 6({\sigma_{xy}}^2 + {\sigma_{yz}}^2 + {\sigma_{zx}}^2)} \qquad (7)$$

Figs.4(a) and (b) show the snapshots of the simulation model before and after the emission of the Shockley partial dislocations. It is clear to see that the grain boundary area shows the largest concentration of stress. The slipping of the dislocation array did not fundamentally change the stress level in the boundary area, and it shows no obvious effect on the stress distribution in the bicrystal system. Therefore, it is reasonable to see a stress plateau at stage-2 in Fig.2. The result has an implication that the non-planar GB structure with dissociated partial dislocations can increase the ductility of the simulated sample under shear. During the emission process in stage-2, the boundary plane rearranged itself by adjusting positions of local atoms. As shown in Fig.3(b), this rearrangement can be regarded as a combination of GB dislocations that described by (1/6)[$\bar{1}\ \bar{1}\ \bar{4}$] + (1/3)[1 1 $\bar{1}$] → (1/6)[1 1 $\bar{6}$].

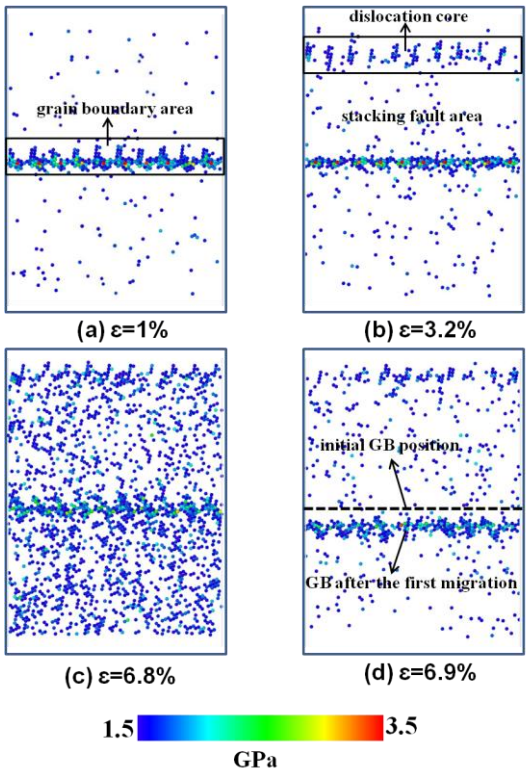

Fig.4 Snapshots of Cu bicrystal model at different deformation stages. Atoms are colored by the value of Von Mises stress where atoms with the stress value less than 1.5 GPa are removed to facilitate the view of stress change within the simulation system.

The propagation of dislocations was blocked when they reached the top fixed area in grain-A. After that, the stress curve reached the strain-hardening stage with a continuous

stress increase without any new deformation mechanisms to release the system stress (see Fig.3(a) at ε=5%). We understand that the blocking of dislocation movement is a limitation of the model size in MD simulations. However, recall that the primary role of grain boundary in ultra-fine or nanocrystalline materials is to block the propagation of the dislocations, which causes the dislocation pile-ups at the grain boundary and result in the increased strength of materials. Therefore, from a physical perspective, the fixed area in the simulation model can be regarded as another grain boundary that blocked the dislocation slipping. This blocking always happens in nanocrystalline materials where the grain boundaries hinder the transmission of dislocations at the boundary and thereby make the materials hard to deform[23, 24].

The strain-hardening stage finished, i.e. the maximum shear stress (σ_m=1.61 GPa) had been reached, when the grain boundary began to migrate, leading to the strain-softening stage. A coupled GB motion was clearly observed at this stage, i.e. the boundary plane moved downwards under the applied shear deformation. At this deformation stage, it is interesting to see that the GB exhibit in a 'stop-and-go' mechanism (see in the supplementary video). As the shear deformation proceeds the GB position remains unchanged for a period ('stop' period), but when the increment of shear strain reaches a certain value, the GB suddenly moves ('go' period). This process is corresponding to the 'stick-slip' behavior of the shear stress, as shown in stage-4 in Fig.2. During the 'stop' period of GB motion, the shear stress increases with the shear strain. An almost linear relationship between the shear stress and shear strain was observed. When the GB moves ('go' period), the shear stress suddenly drops from the peak value to the local minimum value. Figs.4(c) and (d) show the stress distribution of the bicrystal system before and after the first jump of GB migration. Obviously, the GB migration played a significant role in accommodating the system stress. The coupled GB motion caused grain-A to grow and grain-B to shrink while once again increasing the length of the intrinsic stacking fault. Fig.3(a)(at ε=9.2%) shows a snapshot of bicrystal configuration after two jumps of GB migration. The original GB position is indicated by the dashed line for comparison.

It is worth noting that, based on the classic theory proposed by Read and Shockley, the non-uniform structure of asymmetric GBs consist of more than two types of dislocations, which can block each other when gliding on the intersection planes and prevent a coupled motion. Therefore, the migration of asymmetric GBs was thought to be impossible, but recent observations of coupled GB motion in bicrystal experiments[25, 26] has suggested that this may not be true. However, the geometric rules of coupling or migration mechanisms of asymmetric GBs are less known. Recently, Trautt et al.[27] studied the stress-driven motion of asymmetrical GBs between cubic crystals over the entire range of inclination angles. Their MD simulations indicated that the dislocations can find a way to glide past each other without completely blocking themselves, so they proposed two mechanisms by which the dislocations could avoid blocking each other, i.e. dislocation reactions and dislocation avoidance[27]. The migration of Σ11(Φ=54.74°) asymmetric GB in the present simulation study also confirmed this view. Simulation result indicates that the GB dislocations could avoid

blocking each other while preserving the total Burgers vector by dislocation reactions. As shown in Fig.3(b)(at ε=9.2%), the GB migrating process was accompanied by the GB dislocation decomposition and combination. This process can be described by: $(1/6)[1\ 1\ \bar{6}] \longleftrightarrow (1/3)[1\ 1\ \bar{2}] + (1/6)[\bar{1}\ \bar{1}\ \bar{2}]$.

4. Summary

Molecular dynamics simulation in this study reported a dual accommodation mechanisms of the Σ11(Φ=54.74°) asymmetric tilt GB at different stress stages, i.e. the emission of dissociated partial dislocations from GB plane and GB migration coupled to shear deformation. The result of this study can provide further information to understand the mechanical behavior of nanocrystalline materials, which is determined by the competition between dislocation activity and GB accommodation of the strain. In addition, the result has a strong implication that the non-planar GB structure with dissociated dislocations can help to increase ductility while retaining the high strength of the nanocrystalline materials. This finding provides the theoretical basis for grain boundary engineering to attain certain bulk polycrystalline properties.

Acknowledgement

This work was supported by Australian Research Council Discovery Projects (DP130103973). The authors would like to acknowledge the financial support from the China Scholarship Council (CSC).

References

[1] Meyers MA, Mishra A, Benson DJ. Mechanical properties of nanocrystalline materials. Progress in Materials Science. 2006;51:427-556.

[2] Dao M, Lu L, Asaro RJ, De Hosson JTM, Ma E. Toward a quantitative understanding of mechanical behavior of nanocrystalline metals. Acta Materialia. 2007;55:4041-65.

[3] Wolf D, Yamakov V, Phillpot SR, Mukherjee A, Gleiter H. Deformation of nanocrystalline materials by molecular-dynamics simulation: Relationship to experiments? Acta Materialia. 2005;53:1-40.

[4] Farkas D. Atomistic simulations of metallic microstructures. Current Opinion in Solid State and Materials Science. 2013;17:284-97.

[5] Van Swygenhoven H, Derlet PM. Grain-boundary sliding in nanocrystalline fcc metals. Physical Review B - Condensed Matter and Materials Physics. 2001;64:2241051-9.

[6] Qi Y, Krajewski PE. Molecular dynamics simulations of grain boundary sliding: The effect of stress and boundary misorientation. Acta Materialia. 2007;55:1555-63.

[7] Ke M, Hackney SA, Milligan WW, Aifantis EC. Observation and measurement of grain rotation and plastic strain in nanostructured metal thin films. Nanostructured Materials. 1995;5:689-97.

[8] Wang YB, Ho JC, Liao XZ, Li HQ, Ringer SP, Zhu YT. Mechanism of grain growth during severe plastic deformation of a nanocrystalline Ni-Fe alloy. Applied Physics Letters. 2009;94.

[9] Cahn JW, Taylor JE. A unified approach to motion of grain boundaries, relative tangential translation along grain boundaries, and grain rotation. Acta Materialia. 2004;52:4887-98.

[10] Cahn JW, Mishin Y, Suzuki A. Coupling grain boundary motion to shear deformation. Acta Materialia. 2006;54:4953-75.

[11] Winning M. In-situ observations of coupled grain boundary motion. Philosophical Magazine. 2007;87:5017-31.
[12] Legros M, Gianola DS, Hemker KJ. In situ TEM observations of fast grain-boundary motion in stressed nanocrystalline aluminum films. Acta Materialia. 2008;56:3380-93.
[13] Zhang L, Lu C, Michal G, Tieu K, Cheng K. Molecular dynamics study on the atomic mechanisms of coupling motion of [0 0 1] symmetric tilt grain boundaries in copper bicrystal. Materials Research Express. 2014;1:015019.
[14] Bachurin DV, Weygand D, Gumbsch P. Dislocation-grain boundary interaction in 〈1 1 1〉 textured thin metal films. Acta Materialia. 2010;58:5232-41.
[15] Zhang L, Lu C, Tieu K. Atomistic Simulation of Tensile Deformation Behavior of Σ5 Tilt Grain Boundaries in Copper Bicrystal. Scientific Reports. 2014;4.
[16] Zhang L, Lu C, Tieu K, Pei L, Zhao X, Cheng K. Molecular dynamics study on the grain boundary dislocation source in nanocrystalline copper under tensile loading. Materials Research Express. 2015;2:035009.
[17] Sansoz F, Molinari JF. Mechanical behavior of Σ tilt grain boundaries in nanoscale Cu and Al: A quasicontinuum study. Acta Materialia. 2005;53:1931-44.
[18] Plimpton S. Fast Parallel Algorithms for Short-Range Molecular Dynamics. Journal of Computational Physics. 1995;117:1-19.
[19] Mishin Y, Mehl MJ, Papaconstantopoulos DA, Voter AF, Kress JD. Structural stability and lattice defects in copper: Ab initio, tight-binding, and embedded-atom calculations. Physical Review B - Condensed Matter and Materials Physics. 2001;63:2241061-22410616.
[20] Peach M, Koehler JS. The forces exerted on dislocations and the stress fields produced by them. Physical Review. 1950;80:436-9.
[21] Stukowski A. Structure identification methods for atomistic simulations of crystalline materials. Modelling and Simulation in Materials Science and Engineering. 2012;20.
[22] Stukowski A, Bulatov VV, Arsenlis A. Automated identification and indexing of dislocations in crystal interfaces. Modelling and Simulation in Materials Science and Engineering. 2012;20.
[23] Yamakov V, Wolf D, Phillpot SR, Mukherjee AK, Gleiter H. Dislocation processes in the deformation of nanocrystalline aluminium by molecular-dynamics simulation. Nature materials. 2002;1:45-8.
[24] Van Swygenhoven H, Weertman JR. Deformation in nanocrystalline metals. Materials Today. 2006;9:24-31.
[25] Molodov DA, Gorkaya T, Gottstein G. Dynamics of grain boundaries under applied mechanical stress. Journal of Materials Science. 2011;46:4318-26.
[26] Syed B, Catoor D, Mishra R, Kumar KS. Coupled motion of [1010] tilt boundaries in magnesium bicrystals. PHILOSOPHICAL MAGAZINE. 2012;92:1499-522.
[27] Trautt ZT, Adland A, Karma A, Mishin Y. Coupled motion of asymmetrical tilt grain boundaries: Molecular dynamics and phase field crystal simulations. Acta Materialia. 2012;60:6528-46.